APPLICATION OF A MULTI-COMPARTMENT PERMEABILITY LIMITED LUNG MODEL TO PREDICT LUNG CONCENTRATIONS OF ANTI-TUBERCULOSIS DRUGS IN VIRTUAL HUMAN SUBJECTS

Lu Gaohua[1], Janak Wedagedera[1], Ben G Small[1], Lisa Almond[1], Klaus Romero[2], Debra Hanna[2], David Hermann[3], Iain Gardner[1], Masoud Jamei[1], Amin Rostami-Hodjegan[1,4]

[1]Certara Limited, John Street, Sheffield, S2 4SU, UK; [2] Critical Path Institute, 1730 E. River Road, Tucson, Arizona, 85718, USA; [3]Certara USA, Inc., 103 Carnegie Center, Suite 300, Princeton, NJ 08540, USA; 4 University of Manchester, Stopford Building, Oxford Road, Manchester M13 9PT, UK

Background

Tuberculosis (TB) remains a major global health problem. According to World Health Organisation (WHO) reports, an estimated 8.6 million people developed TB and 1.3 million died from the disease in 2012 [1]. Current therapies for pulmonary TB use combinations of orally dosed drugs that need to reach adequate concentrations in the lungs of infected individuals to achieve therapeutic benefit. The ability to predict lung concentration of anti-TB drugs primarily from *in vitro* experiments would be of great benefit in screening new drug candidates and designing appropriate dosing regimens for novel TB drugs.

Objectives

The aim of this study was to develop a physiologically-based pharmacokinetic (PBPK) model to predict the concentration of different anti-TB drugs in the human lung.

Methods

- Simulations were conducted in the Simcyp simulator V14 R1 (Simcyp LTD, Sheffield, UK)
- The structure of the lung model is shown in Figure 1.

Model assumptions

- Each compartment is homogeneous, with constant physiological and pharmacological parameters.
- No fluid or mucus moves from the lobes to the airways.
- Inhaled air contains no drug whilst exhaled air contains drug with the same concentration as the upper airway air (UAA) compartment.
- Drugs passively diffuse (CL_{PD}) between compartments within a segment and active uptake (CL_{uptake}) and efflux transporters (CL_{efflux}) at the basal (mass-blood) and apical (fluid-mass) membranes of the tissue mass compartments are considered.
- Metabolism(CL_{met}) can occur in tissue mass compartments.
- Immediate equilibrium, defined by the air:fluid partition coefficient (K_{AF}), is assumed between the fluid and air compartments of each segment.
- Simulations were conducted for rifampicin, ethambutol, isoniazid, and pyrazinamide where concentrations in human ELF, plasma and alveolar macrophages or bronchial tissue have been published [2-6].
- Model performance was verified by comparing simulation results with clinical observations.
- The default compound file for multiple dose rifampicin in Simyp V14 was used. Data used to construct compound files for isoniazid, pyrazinamide and ethambutol is shown in Table 1.
- Measured values of unbound fraction in lung tissue homogenate could not be found for any of the compounds, so fu in lung tissue mass was calculated in an analogous manner to that used previously in the liver [7].
- Predicted fu lung mass values are: Rifampicin (0.058), isoniazid (0.984), ethambutol (0.451), pyrazinamide (0.985).
- An *in vitro:in vivo* extrapolation approach was used to predict drug permeability in the lung model accounting for the difference in the surface area of the lung (1-2 m^2 in the upper airways and 140 m^2 in the deep lung) compared to the surface area of the *in vitro* system.
- For rifampicin (0.0169 x 10^{-4} cm/s; [8]) apparent permeability data is available in Calu-3 cells. The apparent permeability data for isoniazid was obtained from published studies in Caco-2 cells [9,10] and for ethambutol and pyrazinamide passive permeability was estimated using a QSAR model (Log Papp Calu-3 cells (10^{-7} cm /s)=0.3345*($LogD_{pH6.5}$) - 0.0956*HDC+1.5539 (r^2=0.73)) (Table 1).

Parameter	Value			Units
	Isoniazid	Ethambutol	Pyrazinamide	
Mol Wt	137.1	204	123.1	(g/mol)
Log P	-0.7	0.059	-0.95	
Compound Type	Monoprotic Base	Diprotic Base	Neutral	
pKa	1.82	9.55, 6.5		
B/P	0.825	1.3	0.63	
fu_p	0.95	0.75	0.9	
fa	1	0.57	0.8	
ka	3.55	0.25	0.9	1/h
fu_{gut}	1	1	0.96	
Q_{gut}	2.39	2.79	2.6	L/h
$P_{eff,man}$	0.318	0.379	0.35	10^{-4} cm/s
V_{ss}	0.5	1.23	0.46	L/kg
CLu_{int} user cytosol	3.125		0.5	µl/min/mg Cytosol
CL_R	2.76	25.55	0.11	L/h
Additional systemic CL		4.35		L/h
Lung effective permeability	0.21	0.479	0.0138	(10^{-4} cm/s)
Lung fu mass	0.984	0.451	0.985	
fu_{fluid}	1	1	1	

Table 1 Compound specific information used to develop PBPK models for isoniazid, ethambutol and pyrazinamide.

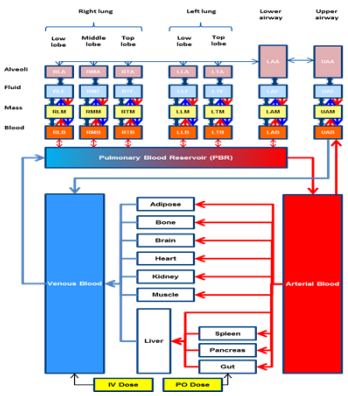

Figure 1. Structure of the multiple-compartment permeability-limited lung model embedded in Simcyp full-PBPK model which consists of 12 perfusion-limited tissue compartments, in addition to the lungs. The lung is approximated by 7 segments, namely, upper (UA) **and** lower (LA) airway**s,** left lung top lobe (LT), left lung low**er** lobe (LL), right lung top lobe (RT), right lung middle lobe (RM) and right lung low lobe (RL). Each of the segments contains 4 compartments representing pulmonary capillary blood, pulmonary tissue mass, fluid and alveoli. In particular, an equibillium is assumed between the fluid and the alveolar air. Within the lung model, the double arrows represent bi-directional passive permeability between adjacent compartments within the same segment, while the unidirectional arrows represent the active transport across the basal and apical membranes of pulmonary tissue. Metabolic elimination exists in the mass compartments.

Results

The simulated and observed ELF:plasma (Figure 2) and alveolar macrophage/tissue :plasma (figure 3) for rifampicin, pyrazinamide, isoniazid and ethambutol. The simulated ELF:plasma ratio in virtual subjects dosed with rifampicin (simulated 0.10-0.17, observed 0.03-0.45) and isoniazid (simulated 0.93 to 1.1, observed 1.2 +/-1.9 in fast acetyators and 3.2+/- 8.1 in slow acetylators) showed overlap with the reported clinical data. For ethambutol the simulated ELF:plasma ratio were of a similar magnitude to (0.4-3.5) the observed clinical values (0.8-1.3) but showed marked inter-individual variability. The simulated ELF:plasma ratio for pyrazinamide was significantly underpredicted (simulated 0.88 to 0.93, observed 11-22).

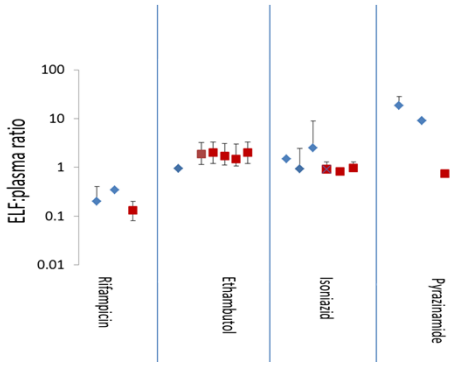

Figure 2 Observed (blue diamonds) and predicted (red square) ELF:plasma ratios for rifampicin, ethambutol, isoniazid, and pyrazinamide. The simulated values are presented as mean value with the range simulated in the virtual population. For rifampicin and pyrazinamide the concentrations in the right lower lobe of the lung are shown. For ethambutol the simulated concentrations are shown (from left to right) for the left upper, left lower, right upper, right middle and right lower lung lobes. For isoniazid the concentrations in the right lower lobe of the lung are shown. The three red squares from left to right represent the concentration in the whole population and in slow and fast acetylators of isoniazid. The average value of the observed clinical data is denoted by a symbol and where it is available the SD has also been shown as a black line (error bar). For some studies only the range of observed values was available and these have been shown on the graph by a dark blue line with no symbol.

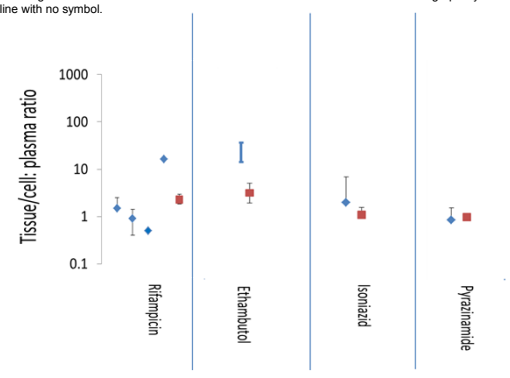

Figure 3 Observed (blue diamonds) and predicted (red square) mean cell or tissue:plasma ratios for rifampicin, ethambutol, isoniazid, and pyrazinamide. The simulated values are presented as mean value with the range simulated in the virtual population. The average value of the observed clinical data is denoted by a symbol and where it is available the SD has also been shown as a black line (error bar). For some studies only the range of observed values was available and these have been shown on the graph by a dark blue line with no symbol.

As shown in Figure 2 for pyrazinamide the simulations underpredicted the observed concentration of the drug in lung ELF. Sensitivity analyses were conducted to look at possible reasons for the underprediction. For a basic drug (pKa 8.99) as the pH in the alveolar lung fluid is decreased the concentration of drug in the fluid is increased so that ELF drug concentrations exceed those in the plasma (figure 4). The systemic plasma and lung mass concentrations are not noticeably affected by the change in lung pH. Figure 5 shows the impact of active efflux from the lung tissue to ELF on simulated ELF concentrations. As the activity of the efflux transporter is increased, the concentration of drug in the ELF increases (Figure 5B) with minimal changes in the drug concentration in the systemic plasma (Figure 5A) or lung tissue (Figure 5C). Given the physicochemical properties of pyrazinamide the effect of an efflux transporter is a possible explanation for the underprediction of ELF concentrations seen for this compound.

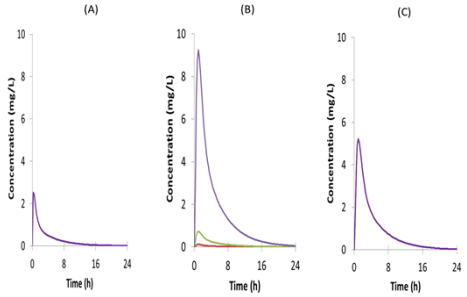

Figure 4 Effect of changing the pH of the epithelial lining fluid of the lung on the concentration of a basic drug (pKa 8.99) in (A) plasma, (B) the lung fluid and (C) the lung mass comaprtments of the lower right lobe lung segment. The pH values used were pH 7.4 (red line), pH 6.6 (green line) and pH 5.5 red line.

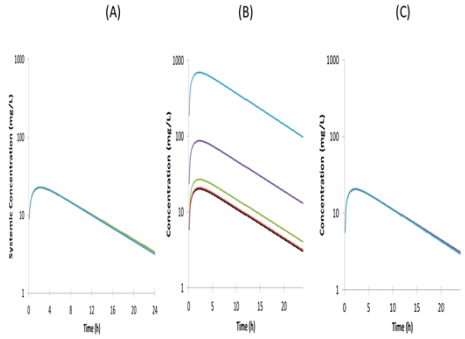

Figure 5 The effect of adding the action of an efflux transporter between the lung mass and epithelial lining fluid on (A) systemic plasma concentration, (B) lung epithelial lining fluid concentration and (C) the lung tissue mass concentration. The clearance of the efflux transporter was set at 0 (black line), 0.06 (red), 0.6 (green), 6 (purple) and 60 L/h (light blue).

Conclusions

- The described lung PBPK model has shown some utility in predicting the lung pharmacokinetics of anti-TB drugs and testing of the model with a wider range of compounds is underway.
- For some compounds assuming purely passive diffusion between the plasma and ELF results in underprediction of the lung fluid concentrations and for these compounds additional processes (eg drug transporters) may be involved.

REFERENCES

[1] World-Health-Organization (2013) http://www.who.int/tb/publications/global_report/en/.
[2] Goutelle et al (2009) Antimicrob Agents Chemother 53:2974-2981.
[3] Conte et al. (1999) Antimicrob Agents Chemother 43:1329-1333.
[4] Conte et al (2001) Antimicrob Agents Chemother 45:2891-2896.
[5] Conte et al (2002) Antimicrob Agents Chemother 46:2358-2364.
[6] Kativar et al (2008) J Postgrad Med 54:245-246.
[7] Jamei et al. (2013)Clin. Pharmacokinetics; 53 :73-87.
[8] Tewes et al., J Control Release. 2008;129(2):93-9.
[9] Goncalves et al., Biopharm Drug Dispos. 2012; 33:316-23.
[10] Ranaldi et al Antimicrob Agents Chemother. 1992; 36(7):1374-81.